

Effects of Carbon-Coated Titanium Dioxide Nanoparticles as a Photostabilizer on the Photodegradation of Rigid Poly(vinyl chloride)

Parvane Sokhandani,^{1,2} Mohammad Adel Abdi,¹ Shadi Ghaebi Mehmandoust,¹ Ali Akbar Babaluo,¹ Reza Mehdizadeh,^{1,2} Mostafa Rezaei,² Masoud Rakhshani^{1,2}

¹Nanostructure Material Research Center, Sahand University of Technology, P.O. Box 51335/1996, Tabriz, Iran

²Institute of Polymeric Materials, Sahand University of Technology, P.O. Box 51335/1996, Tabriz, Iran

Correspondence to: A. A. Babaluo (E-mail: a.babaluo@sut.ac.ir)

ABSTRACT: In this study, nanocomposites of rigid poly(vinyl chloride) (UPVC) using the synthesized carbon-coated titanium dioxide (TiO₂) nanoparticles and commercial powder of titanium dioxide (with rutile structure) were prepared by melt blending. The presence of carbon-coated TiO₂ nanoparticles with rutile structure in UPVC matrix led to an improvement in photo stability of UPVC nanocomposites in comparison with commercial UPVC. The photocatalytic degradation behavior of nanocomposites was investigated by measuring their structural changes, surface tension, and mechanical and morphological properties before and after UV exposure for 700 h. It was found that mechanical and physical properties of UPVC nanocomposites are not considerably reduced after UV exposure in the presence of carbon-coated TiO₂ nanoparticles even in small percentage of nanoparticles in comparison with the presence of commercial TiO₂ particles. Therefore, it can be concluded that UPVC/TiO₂ nanocomposite with low content of carbon-coated TiO₂ nanoparticles (0.25 wt %) illustrated high stability under light exposure. © 2013 Wiley Periodicals, Inc. *J. Appl. Polym. Sci.* 2014, 131, 40228.

KEYWORDS: mechanical properties; degradation; irradiation; poly(vinyl chloride); morphology

Received 1 August 2013; accepted 26 November 2013

DOI: 10.1002/app.40228

INTRODUCTION

Poly(vinyl chloride) (PVC) is one of the most important and widely in use thermoplastics because of its valuable properties, such as low production cost, good process ability, easy modification, and excellent chemical and fire resistance.^{1,2} The ultimate user acceptance of PVC products for outdoor building applications will depend on their stability to resist deterioration of their mechanical and aesthetic properties over long periods of exposure that is needed to a careful compounding.^{3,4} Because, the energy content of ultraviolet (UV) region can rupture the most chemical bonds of polymer structure⁵; therefore, these PVC products are degraded under sun's UV radiation⁶ which leads to severe discoloration and loss of mechanical properties of these products.⁵ The photodegradation of PVC is complex and not completely understood due to coexistence of dehydrochlorination (HCl elimination) and oxidation reactions.⁷ Therefore, study on the photodegradation of such products still remains a matter of interest.

One of the major UV stabilizers is titanium dioxide (TiO₂). There is a large amount of literatures regarding the photodegradation of PVC and the effects of TiO₂ on its degradation.^{8–14} Real et al.⁸ investigated the influence of the combined action of

water, temperature, and radiation in the oxidative ageing by means of infrared spectroscopy. Also, Real et al.⁹ investigated the photo-oxidation of PVC by following the formation of oxidation products of the carbonyl groups using Fourier transfer infrared (FTIR) measurements. Gardette and Lemaire¹⁰ studied the influence of photo-catalytic pigments (zinc oxide and two rutile forms of TiO₂) on the changes in the FTIR spectra of irradiated samples where no noticeable photo-catalytic effect of the pigments was observed. Furthermore, they¹¹ studied the mechanisms of photochemical and thermal oxidations of PVC, and the products formed during the photolyzing of PVC in the presence or absence of oxygen was investigated by UV-visible and FTIR spectroscopies. Anton-Prinet et al.¹² investigated the effect of TiO₂ pigment on the formation of degradation products. They confirmed that the thickness of the degraded layer is lower for pigmented sample (200 μm) than that for unpigmented one (400 μm).

Therefore, TiO₂ can be considered as an effective absorber over the whole UV range¹³ which can substantially reduce depth of penetration of UV radiation into the PVC bulk and consequently decrease its degradation.¹² Conversely, carbon is an effective UV absorber and carbon-coated TiO₂ have very good

Table I. Composition of the Prepared UPVC Nanocomposites

Name	PVC (phr)	Commercial TiO ₂ (phr)	Carbon-coated TiO ₂ (phr)	Chlorinated polyethylene (phr)	CaCO ₃ (phr)	CaSt ₂ (phr)	ZnSt ₂ (phr)	Paraffin wax (phr)	StAc (phr)
CP	100	3.4	-	3.7	8	2.5	2.5	2.8	0.22
NP1	100	3.3	0.1	3.7	8	2.5	2.5	2.8	0.22
NP2	100	3.15	0.25	3.7	8	2.5	2.5	2.8	0.22
NP3	100	2.9	0.5	3.7	8	2.5	2.5	2.8	0.22
NP4	100	2.4	1	3.7	8	2.5	2.5	2.8	0.22

capability to absorb UV radiation.¹⁵ But, the effect of the carbon-coated TiO₂ nanoparticles on the photostabilization of unplasticized PVC (UPVC) has not been investigated precisely. Furthermore, the mechanical and chemical properties of the samples could severely be changed under photodegradation process,⁷ but few publications concerning the effect of the photodegradation on the mechanical and chemical properties of UPVC have been reported.

In this study, the effects of carbon-coated TiO₂ nanoparticles with rutile structure on the photo stabilization of UPVC were investigated. UPVC nanocomposites were prepared by melt-compounding at the presence of the commercial TiO₂ with rutile structure and synthesized carbon-coated TiO₂ nanoparticles with rutile structure. It should be mentioned that in this work, the commercial formula of UPVC/TiO₂ nanocomposite was used for preparing the nanocomposites, and then the results were compared with commercial samples. The effect of the synthesized TiO₂ nanoparticles on the photostabilization of UPVC was investigated by morphological studies and measuring the carbonyl groups and carbon-carbon double bonds in UPVC by FTIR measurements compared to commercial TiO₂ composite. As well as the effect of TiO₂ nanoparticles on the physical and mechanical properties of UPVC (nano)composites before and after photodegradation was investigated.

EXPERIMENTAL

Materials

PVC (Bandar Imam Petro, Iran) (*K* value 64–66) as polymer matrix, two different titanium dioxide (TiO₂): commercial rutile particles (Mapa-Trans, Ukraine) and homemade carbon-coated rutile nanoparticles^{16–18} as UV absorbers, calcium carbonate (CaCO₃) (Poodrkar, Iran) as filler, chlorinated polyethylene (CPE) (Poodrkar, Iran) as impact modifier, calcium stearate (CaSt₂) and zinc stearate (ZnSt₂) (Poodrkar, Iran) as thermal stabilizer, paraffin wax (Poodrkar, Iran) as internal lubricant, and stearic acid (StAc) (EPS IMPEX, Malaysia) as external lubricant were used to prepare PVC nanocomposite compounds.

Preparation of UPVC/TiO₂ Nanocomposites

PVC nanocomposites were prepared according to Table I. To evaporate moisture and prepare homogeneous compounds, dry powder blends were premixed and heated from room temperature to 120°C over approximately 12 min. Dry blends were processed using an internal mixer (Brabender, W50EHT, Plasti-

cor, Germany) (with a rotor speed of 60 rpm), and temperature of 170°C for 8 min. The resulting compound was then molded into rectangular sheets by compression molding at 170°C and 5 MPa pressure for 5 min using a hot press (Brabender, Polystat 200 T, Germany).

Artificial Weathering

The artificially simulated weathering was performed using two different light source chambers. The first chamber was equipped with a (TL 20 W/05, Philips, Germany) ultraviolet (UV) exposure lamp with a maximum emission at 365 nm. Another one was equipped by a (HQI-TS 150 W/NDL, Osram, Germany) visible (Vis) exposure lamp with a maximum emission at 590 nm, with a fan to have the same temperature ranges in both chambers. The relative humidity was 60–70% and the temperature was 25°C in the chambers. The irradiation distance between the lamp and the samples was 25 cm.

Characterization

Characterization of Carbon-Coated and Commercial TiO₂ (Nano)particles. Nitrogen adsorption analysis (BET) was performed with CHEMBET-3000 apparatus. The surface morphology of (nano)particles was examined using VEGA\\TESCAN scanning electron microscopy (SEM). XRD patterns of TiO₂ (nano)particles were performed on a Siemens D5000 X-ray diffractometer (XRD) using CuK α radiation. The UV and visible spectra of (nano)particles were performed on a PERKIN ELMER UV-Vis recording spectrophotometer. The size and uniformity of (nano)particles were examined by particle size analyzer apparatus (FRITSCH, Analysette 22 NanoTec).

Characterization of UPVC/TiO₂ Nanocomposites. Tensile test measurements. Tensile tests were performed at room temperature (25°C) according to ASTM D638 using the tensile testing machine (Zwick-Roell Z010). The samples before and after irradiation were tested at a crosshead speed of 10 mm/min. The reported values are the average of six measurements on specimens were taken from the same direction of molded samples.

FTIR spectroscopy. Fourier transform infrared (FTIR) analysis was performed at room temperature (25°C) using the FTIR spectrometer (UNICAM Matson 100, England). Samples were tested before and after UV and visible light irradiation to assess the extent of degradation in the nanocomposites. The IR spectra were recorded in absorbance mood from the 1500–1900 cm⁻¹ range; the peak area of the carbonyl and polyene bands was used to estimate photodegradation using the Essential FTIR software (Operant LLC, Version 1.1.0.0).

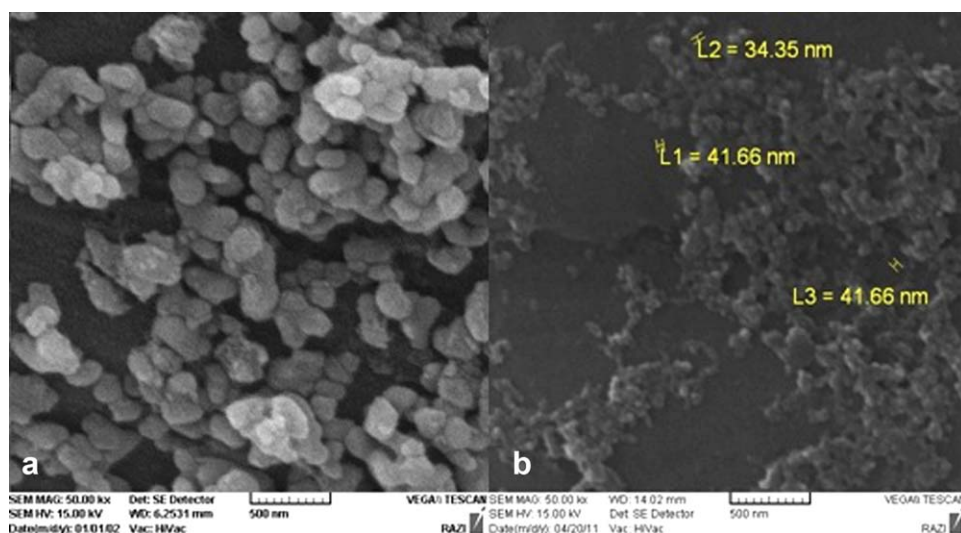


Figure 1. SEM micrographs of: (a) commercial TiO_2 . (b) Carbon-coated TiO_2 nanoparticles. [Color figure can be viewed in the online issue, which is available at wileyonlinelibrary.com.]

Contact angle measurement. Contact angles of two liquids (normal decane and deionized water) on PVC film before and after irradiation were measured at room temperature (25°C), with contact angle measurement apparatus made in our laboratory, equipped with optical microscope (TZM-2 model, BEL, Italy). The liquid droplet ($2\ \mu\text{L}$) was placed onto the polymer surface by a micro syringe. The droplet image was recorded, and then contact angle of each drop was measured by Image-J software. Each contact angle is the average of minimum five measurements. The surface tension (γ_s) and their dispersive (γ_s^D) and polar (γ_s^P) components were calculated using the Fowkes methods.¹⁹

Morphology analyses. The surface morphology of UPVC (nano)composites before and after UV and visible irradiation was examined using VEGA\\TESCAN SEM.

RESULTS AND DISCUSSION

Nanoparticles Properties

Figure 1 shows the SEM micrographs of the (nano)particles. The SEM micrographs confirm the nanometric size of synthesized nanoparticles.

Figure 2 shows the particle size analysis of (nano)particles. The average size of carbon-coated TiO_2 nanoparticles is equal 26 nm and the average size of commercial rutile particles is 540 nm confirming the results of SEM micrographs. The uniformity of carbon-coated nanoparticles is 37.91 that higher than uniformity of commercial particles (5.02).

The carbon content of the synthesized TiO_2 nanoparticles was determined by thermogravimetry and the results are presented

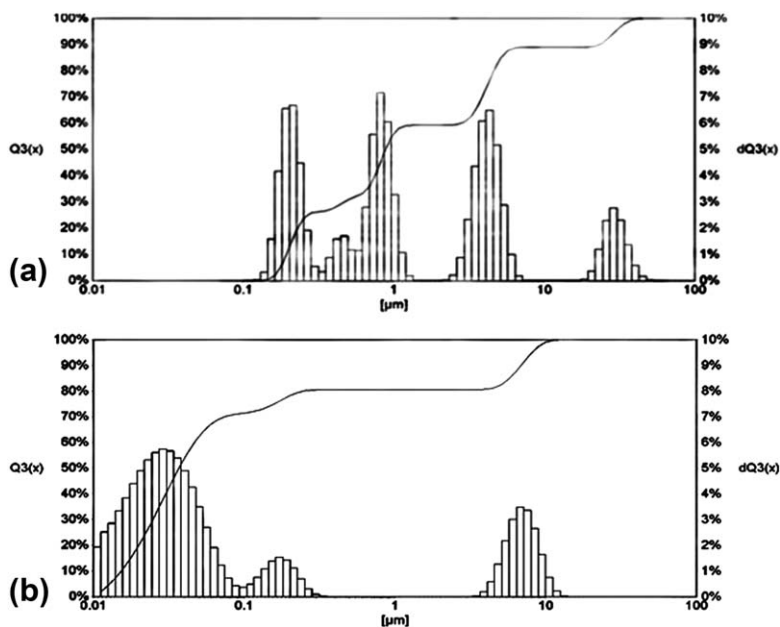


Figure 2. Particle size analysis of: (a) commercial TiO_2 . (b) Carbon-coated TiO_2 nanoparticles.

Table II. Carbon Content and Specific Surface Area of TiO₂ (Nano) Particles

Sample	Carbon content (%)	Specific surface area (m ² /g)
Commercial TiO ₂		12.4
Carbon-coated TiO ₂	3.46	73.4

in Table II, as well as the specific surface area of the TiO₂ (nano)particles is reported in Table II.

Figure 3 shows UV–Vis spectra of carbon-coated TiO₂ nanoparticles and commercial TiO₂ particles. These spectra show that carbon-coated TiO₂ nanoparticles have high ability of UV and visible light absorption compared to commercial particles. The reason of this ability can be due to the presence of carbon in structure of the synthesized nanoparticles.²⁰

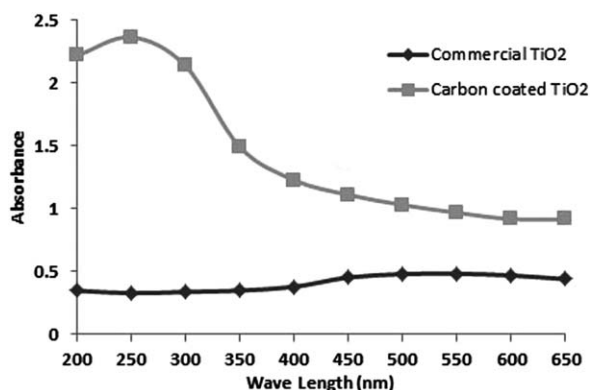
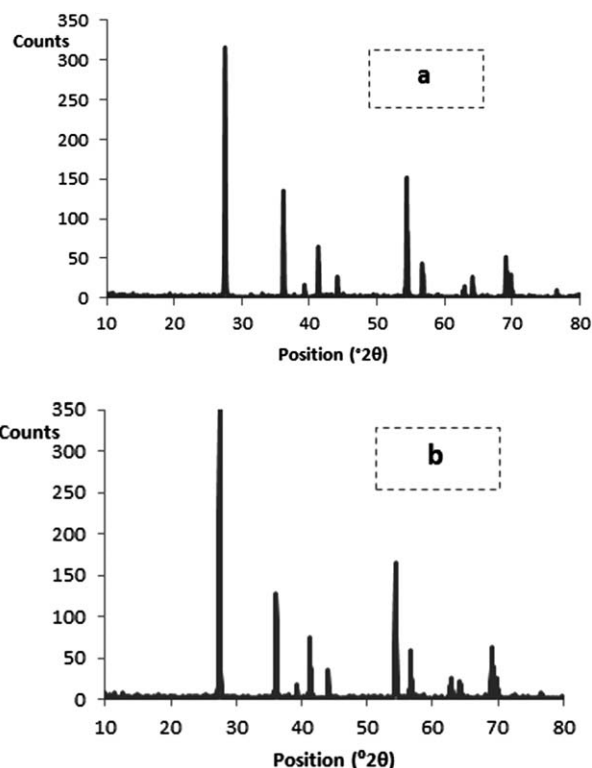
Figure 4 shows XRD patterns of carbon-coated TiO₂ nanoparticles and commercial TiO₂ particles confirming the single phase of rutile crystalline structure of TiO₂.

PVC Nanocomposites

Morphological Study of Nanocomposites. Figures 5 and 6 show the surface micrographs of the UPVC nanocomposites that were irradiated under UV and visible light exposure for 700 h in the presence of air. Furthermore, the Figure 7 shows the SEM micrographs of UPVC (nano)composites that were irradiated under sun light exposure for 3000 h.

The SEM micrographs reveal that the photocatalytic degradation of PVC leads to the formation of micrometer size cavities that might be induced by the escape of HCl during the elimination reactions or other volatile degradation products from PVC matrix.

As it can be seen, degradation intensities of nanocomposites consisting of carbon-coated nanoparticles are significantly lower than CP sample that consists of commercial TiO₂ particles. Despite of CP composite, the pits are developed during the exposure, the nanocomposites consisting of carbon-coated TiO₂ nanoparticles show the higher resistance. This trend can confirm the high absorption of UV and visible light of nanopar-

**Figure 3.** UV–Vis spectrum of carbon-coated TiO₂ nanoparticles and commercial TiO₂ particles.**Figure 4.** XRD patterns of: (a) commercial TiO₂. (b) Carbon-coated TiO₂ nanoparticles.

ticles in the presence of carbon layer. Another factor of high resistance of nanocomposites can be attributed to the hydrophobic property of carbon-coated TiO₂ nanoparticles. In the commercial composite, TiO₂ particles have hydrophilic property that this feature can lead to create the hydrogen free radicals in the polymeric matrix during processing.²¹ But in carbon-coated TiO₂ nanoparticles, the presence of carbon can decrease the hydrophilic property of dioxide titanium so degradation intensity of nanocomposites is decreased.

Finally, it can be concluded that, at the instant of UV and visible light irradiation, commercial composite consisting of TiO₂ particles with rutile structure undergoes a higher degradation compared to nanocomposites that include carbon-coated TiO₂ nanoparticles even in the small percentage of nanoparticles, because rutile structure and presence of carbon can intensify photostabilization of UPVC/TiO₂ nanocomposites.

FTIR Analyses of Nanocomposites. The functional groups in the nanocomposite films were monitored by FTIR analysis. Figure 8 shows the changes in the FTIR spectra of the nanocomposite films before and after UV and visible light exposure. The main differences that were observed in these absorption spectra are related to the polyene (1600–1680 cm⁻¹) and carbonyl (1680–1780 cm⁻¹) groups. For all the nanocomposites films, intensities of the polyene and carbonyl groups absorption peaks increase after irradiation time. Furthermore, polyene index was calculated by subtracting the value of the integrated surface area of the absorption bands at 1630 cm⁻¹ from the baseline and dividing it by the reference value of the integrated surface area

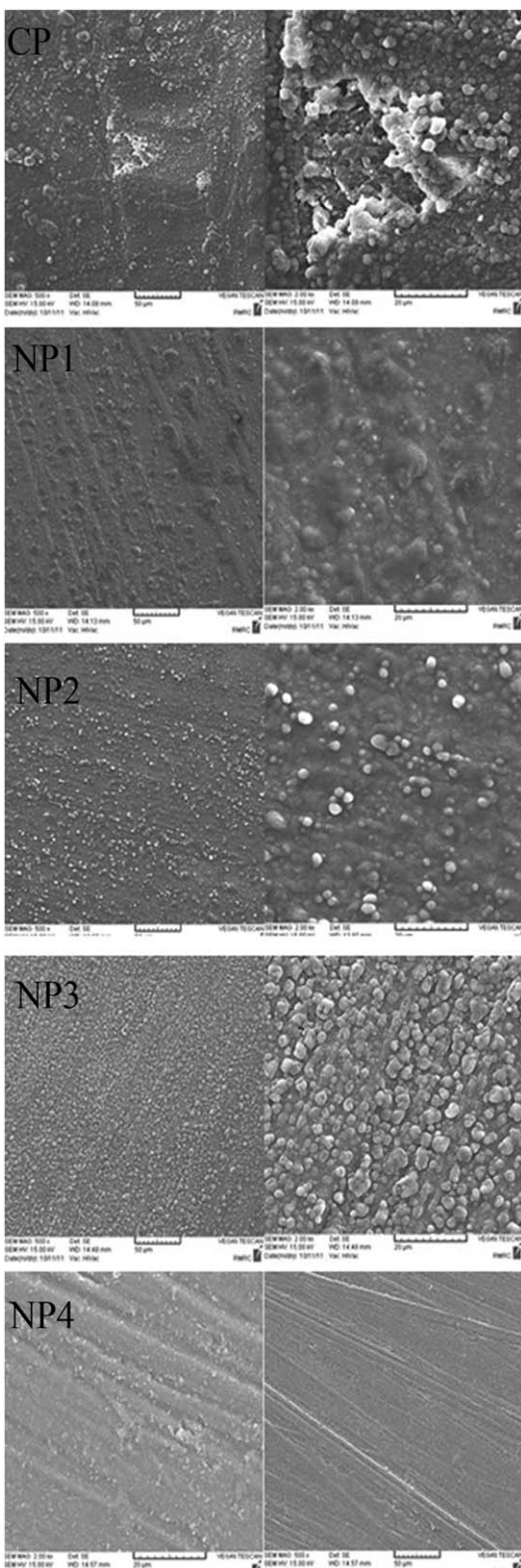


Figure 5. SEM micrographs of UPVC (nano)composites after 700 h of UV irradiation with different magnification.

of the absorption bands at 2920 cm^{-1} subtracted from the baseline as shown in eq. (1).^{22,23} The different wave numbers followed were 2920 and 1650 cm^{-1} for C—H stretching and

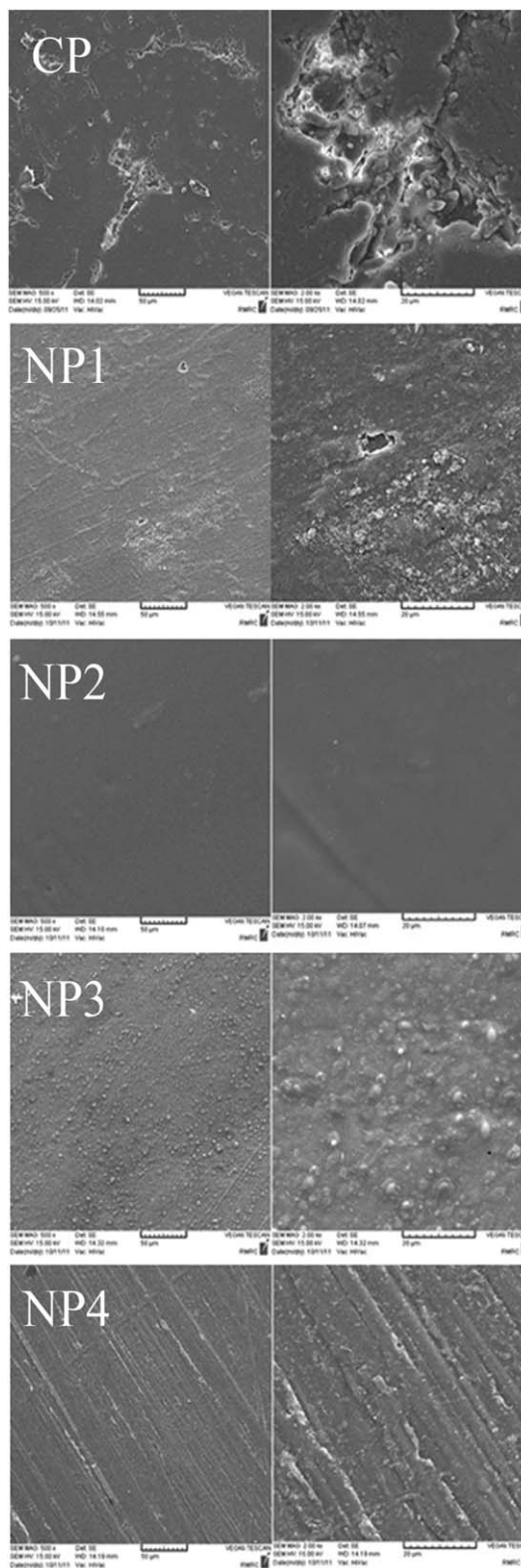


Figure 6. SEM micrographs of UPVC (nano)composites after 700 h of visible light irradiation with different magnification.

polyene sequences, respectively. For carbonyl index, it was calculated according to eq. (2). The wave number of 1730 cm^{-1} represents carbonyl groups; where A_{1730} is the integrated

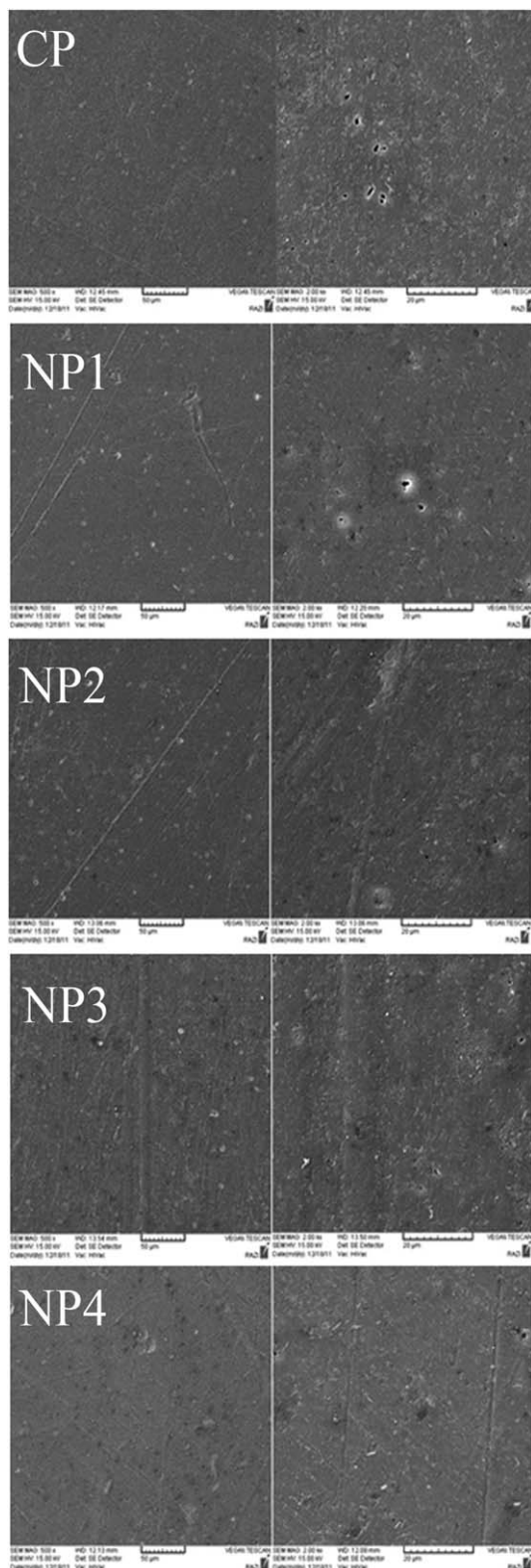


Figure 7. SEM micrographs of UPVC (nano)composites after 3000 h of natural irradiation with different magnification.

surface area of the absorption bands at 1730 cm^{-1} . The results of calculated polyene and carbonyl indexes are presented in Figures 9 and 10.

$$\text{Polyene index} = \frac{(\%A_{1650} - \%A_{\text{baseline}})}{(\%A_{2920} - \%A_{\text{baseline}})} \quad (1)$$

$$\text{Carbonyl index} = \frac{(\%A_{1730} - \%A_{\text{baseline}})}{(\%A_{2920} - \%A_{\text{baseline}})} \quad (2)$$

As can be seen in the Figures 9 and 10, the polyene and carbonyl indexes for nanocomposites increase after irradiation. The increase in polyene sequences can probably due to a photodegradation of UPVC nanocomposites. Furthermore, the increasing intensities of the carbonyl groups suggest that the photooxidation reaction has taken place in the composite film. In the composite film, TiO_2 nanoparticles can be excited by UV light to generate active electron-hole pairs, which can react with the surface-absorbed molecules and form active oxygen species. Then, these active oxygen species oxidize C-H groups to form C=O groups.²⁴ In

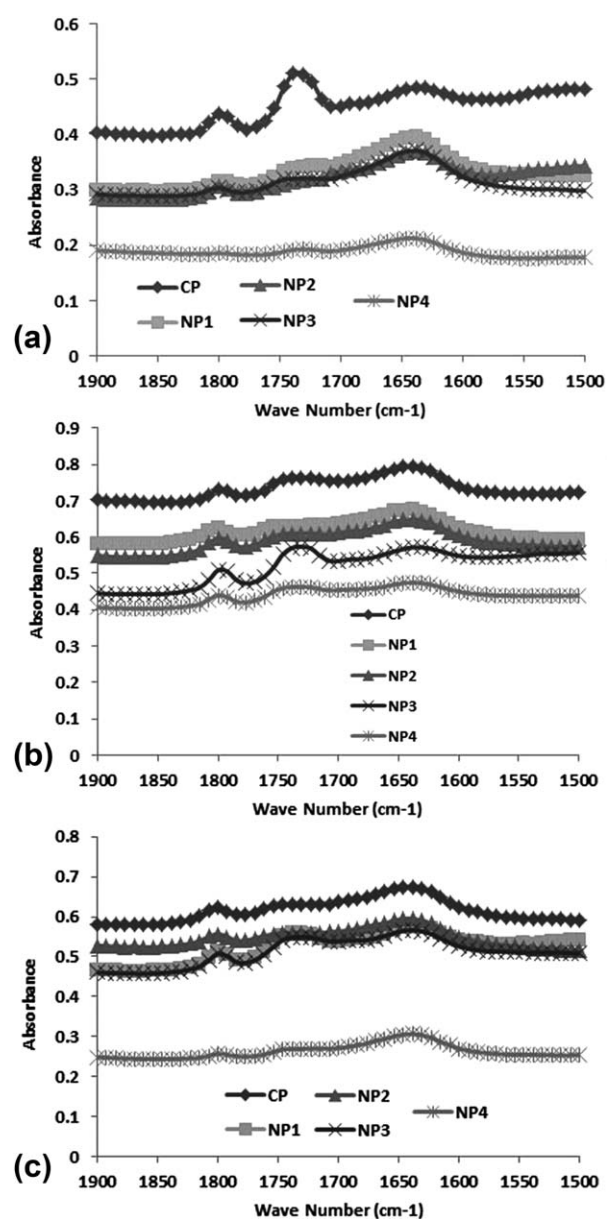


Figure 8. FTIR spectra of (nano)composites: (a) before exposure, (b) after UV exposure, (c) after visible light exposure.

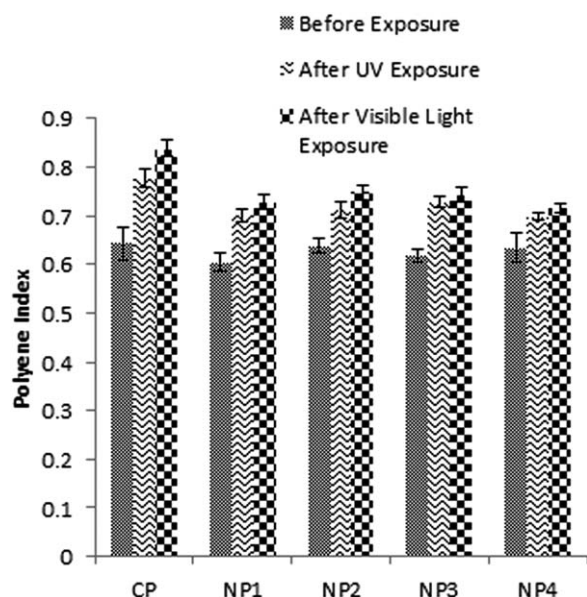


Figure 9. Polyene index of (nano)composites before and after UV and visible light exposure.

nanocomposites with carbon-coated TiO₂ nanoparticles, the rate of photodegradation is much lower than commercial composite (CP). The lower ratio of photodegradation products in nanocomposites is due to the high absorbance ability of nanoparticles that act as UV stabilizer and lead to the low UV penetration depth and decrease formation of double bonds in UPVC matrix. Furthermore, the carbon-coated TiO₂ nanoparticles have lower activity in creating active oxygen species compared to commercial TiO₂ particles because the presence of carbon can decrease the rate of oxidation reactions and this issue leads to decreasing the rate of carbonyl groups in UPVC/TiO₂ nanocomposites.²⁵ So, this means the photostability of UPVC in the presence of carbon-coated TiO₂ nanoparticles increases.

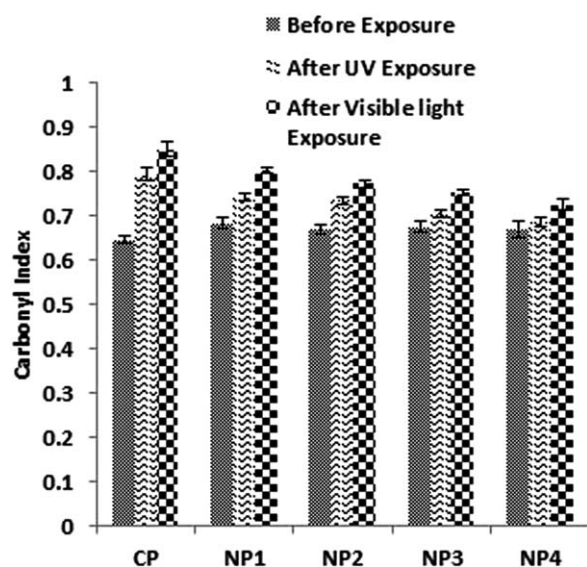


Figure 10. Carbonyl index of (nano)composites before and after UV and visible light exposure.

Table III. Contact Angle Values for Samples with Different Solvents Before and After UV Exposure

Sample	Exposure mode	Contact angle (°)	
		Water	<i>n</i> -Decane
CP	Before	84.7	20.5
	After	62.5	23.5
NP1	Before	88.9	20.1
	After	82.9	22.3
NP2	Before	89.9	20.5
	After	84.1	22.7
NP3	Before	90.1	21.3
	After	84.6	23.1
NP4	Before	90.9	21.8
	After	86.6	23.6

Contact Angle of Nanocomposites. The method of static contact angle (θ) (Sessile drop) measurement was used to calculate the polymer surface tension. The changes in the contact angle and surface tension in UV-irradiated nanocomposites are presented in Tables III and IV. Contact angle is a measure of non-covalent forces between liquid and the first monolayer of material. Thus, in the case of strong interaction between phases, the liquid drop spreads on the solid and wets it. The quality of the surface, its roughness, and porosity strongly influence contact angle values. The wettability of *n*-decane on PVC is much higher (small θ values) than water (higher θ values), because the molecules of a highly polar liquid are less attracted by PVC macromolecules, which has a relatively low polarity. The results of the contact-angle measurements were analyzed according to the Young theory to estimate dispersive and polar components of the samples surface tension.^{4,26}

In accordance to Table III, the contact angle values show a decrease for water and an increase for *n*-decane, as a solvent, after UV exposure. A decrease in contact angle values demonstrated on better dispersion of solvent on the surface and the better dispersion means better consistency with surface. As it is

Table IV. Surface Tension of Samples Obtained from Contact Angle Values

Sample	Exposure mode	γ_S^P (mJ/m ²)	γ_S^D (mJ/m ²)	γ_S (mJ/m ²)
CP	Before	6.1	22.3	28.4
	After	19.3	21.8	41.1
NP1	Before	4.4	22.4	26.7
	After	7.1	22.1	29.1
NP2	Before	4.1	22.3	26.4
	After	6.5	21.9	28.5
NP3	Before	4.0	22.2	26.2
	After	6.3	21.9	28.3
NP4	Before	3.7	22.1	25.8
	After	5.5	21.8	27.3

Table V. Mechanical Properties of UPVC (Nano)composites Before and After 700 h of UV Irradiation

	Before exposure					After exposure				
	CP	NP1	NP2	NP3	NP4	CP	NP1	NP2	NP3	NP4
Elastic modulus (MPa)	2118	2602.7	2631.7	2655	2700	2493.3	2652.7	2681	2730	2818.3
Elongation at break (%)	111.2	115.6	125.6	127.5	127.8	17	53.5	58.9	79.2	81.2
Tensile strength (MPa)	60.6	65.2	65.7	66.8	67.9	50.4	57.3	59.3	63.5	63.2
Yield stress (MPa)	57.6	64.3	67	68.1	69.2	67.5	70.7	76.4	76.2	70.2

known, water is a polar and *n*-decane is a non-polar fluid, therefore the trend from contact angle measurements confirms increasing of surface hydrophilicity after UV exposure. But as can be observed in Table IV, after UV exposure to the samples, the dispersive component of surface tension shows a little decrease although the polar component increases significantly. So, variation in surface tensions values comes from the changes in their polar component. This increase in surface tensions demonstrated an increase on polarity of surface; which is attributed to the formation of polar groups and enrichment of surface with functional groups.²⁷ This significant increase of PVC polarity indicates that an efficient oxidation on polymer surface occurs. The polymer surface is activated by UV irradiation, which explains such efficient oxidation. This leads to the formation of different types of carbonyl, hydroxyl, and hydroperoxide groups that strongly influences γ_S^P and γ_S^D , therefore encounter more hydrophilicity to the samples after UV exposure. Another reason is the possibility of formation of small cracks, crazes, and voids, after UV exposure which influences the contact angle measurements. In nanocomposites decrease in contact angle and surface tension is less than that in commercial composite. These results reveal good photostability potential of these nanocomposites in comparison with CP composite, as mentioned in Morphological Study of Nanocomposites section. This behavior can be related to the high UV absorption as well as hydrophobic property of carbon-coated TiO₂ nanoparticles.²¹ These results are in good agreement with morphological and structural measurement results.

Mechanical Properties of Nanocomposites. Table V represents the elastic modulus of UPVC/TiO₂ (nano)composites before and after UV exposure. As can be seen in Table V, the elastic modulus of nanocomposites is higher than commercial composite, the reason of this increasing can be attributed to the better dispersion of carbon-coated nanoparticles in UPVC matrix and more effective interactions between the filler and matrix.²⁸ The results showed an increment in the (nano)composites modulus after UV irradiation which can be related to the formation of crosslinking in UPVC structure during the photodegradation. The results revealed that the highest elastic modulus increment resulted from the highest photodegradation was occurred in commercial composite.

The results of elongation at break for the (nano)composites at the presence of carbon-coated TiO₂ nanoparticles and commercial TiO₂ particles before and after UV exposure are presented in Table V. The results reveal a considerable decrease in elonga-

tion at break in CP sample after UV exposure, but nanocomposites containing carbon-coated TiO₂ nanoparticles show the highest resistance after UV exposure. This decreasing can be assimilated to a ductile to brittle transition spread over time.⁴ But the presence of carbon-coated TiO₂ nanoparticles in UPVC matrix results in a significant decrease of the elongation at break reduction because of high UV absorption of nanoparticles. This fact is very important in manufacturing of photo stable outdoor UPVC articles.

Table V represents the tensile strength of (nano)composites. In these samples, there is no significant difference in tensile strength which is very crucial for preparing of photostable UPVC articles. A similar behavior is observed in Table V for yield stress of (nano)composites.

CONCLUSION

UPVC nanocomposites filled with different types of TiO₂ (carbon-coated nanoparticles and commercial particles) with rutile structure were prepared via melt blending method. The results of tensile measurements showed that the presence of carbon-coated TiO₂ nanoparticles led to an improvement in photostability of UPVC nanocomposite in comparison with commercial UPVC composite after UV exposure. The contact angle and surface tension measurement results indicated that increase in the polar component (γ_S^P) of UPVC is attributed to the formation of polar groups in the photodegraded UPVC after exposure. But this increasing in the polar component is not significant in UPVC nanocomposites with the presence of carbon-coated TiO₂ nanoparticles even in small percentages (0.25 wt %) of these nanoparticles compared to those with commercial TiO₂ particles. Furthermore, the results of the FTIR analyses and morphological properties confirmed this consequence. The obtained results illustrated that the samples consist of carbon-coated titanium dioxide nanoparticles have higher photostability which can be due to high UV and visible light absorption of the nanoparticles.

REFERENCES

- Kaczmarek, H.; Kowalonek, J.; Oldak, D. *Polym. Degrad. Stab.* **2003**, *79*, 231.
- Kaczmarek, H.; Swiatek, M.; Kaminska, A. *Polym. Degrad. Stab.* **2004**, *83*, 35.

3. Pimentel Real, L. E.; Ferraria, A. M.; Botelho do Rego, A. M. *Polym. Test.* **2008**, *27*, 743.
4. Sokhandani, P.; Babaluo, A. A.; Rezaei, M.; Shahrezaei, M.; Hasanzadeh, A.; Ghaebi Mehmandoust, Sh.; Mehdizadeh, R. *J. Appl. Polym. Sci.* **2013**, *129*, 3265.
5. Kamisli, F.; Turan, C. *J. Mater. Proc. Technol.* **2005**, *159*, 40.
6. Zeng, X. F.; Wang, W. Y.; Wang, G. Q.; Chen, J. F. *J. Mater. Sci.* **2008**, *43*, 3505.
7. Real, L. P.; Rochaa, A. L. P.; Gardette, J. L. *Polym. Degrad. Stab.* **2003**, *82*, 235.
8. Real, L. P.; Gardette, J. L.; Rocha, A. P. *Polym. Degrad. Stab.* **2005**, *88*, 357.
9. Real, L. E. P.; Ferraria, A. M.; Rego, B. D. *Polym. Test.* **2008**, *27*, 743.
10. Gardette, J. L.; Lemaire, J. *Polym. Degrad. Stab.* **1991**, *33*, 77.
11. Gardette, J. L.; Lemaire, J. *Polym. Degrad. Stab.* **1991**, *34*, 135.
12. Anton-Prinet, C.; Mur, G.; Gay, M.; Audouin, L.; Verduc, J. *Polym. Degrad. Stab.* **1998**, *61*, 211.
13. Jin, C. Q.; Christensen, P. A.; Egerton, T. A.; White, J. R. *Mater. Sci. Technol.* **2006**, *22*, 908.
14. Choi, W.; Kim, S.; Cho, S.; Yoo, H.; Kim, M. H. *Korean J. Chem. Eng.* **2001**, *18*, 898.
15. Zhang, L. W.; Fu, H. B.; Zhu, Y. F. *Adv. Funct. Mater.* **2008**, *18*, 2180.
16. Tahmasebpour, M.; Babaluo, A. A.; Razavi Aghjeh, M. K. *J. Eur. Ceram. Soc.* **2008**, *28*, 773.
17. Tahmasebpour, M.; Babaluo, A. A.; Shafiei, S.; Pipelzadeh, E. *Powder Technol.* **2009**, *191*, 91.
18. Rakhshani, M.; Kamrannejad, M. M.; Babaluo, A. A.; Rezaei, M.; Razavi Aghjeh, M. K. *Iran. Polym. J.* **2012**, *21*, 821.
19. Comyn, J.; Blackley, D. C.; Harding, L. M. *Int. J. Adhes. Adhes.* **1992**, *13*, 63.
20. Valentin, C.; Pacchioni, G.; Selloni, A. *Chem. Mater.* **2005**, *17*, 6656.
21. Tryba, B. *Int. J. Photoenergy* **2008**, *2008*, ID 721824.
22. Chaochanchaikul, K.; Sombatsompop, N. *Polym. Eng. Sci.* **2011**, *51*, 1354.
23. Shi, W.; Zhang, J.; Shi, X. M.; Jiang, G. D. *J. Appl. Polym. Sci.* **2008**, *107*, 528.
24. Yang, C.; Deng, K.; Peng, T.; Zan, L. *Chem. Eng. Technol.* **2011**, *34*, 886.
25. Chen, X.; Mao, S. S. *Chem. Rev.* **2007**, *107*, 2891.
26. Kaczmarek, H.; Kowalonek, J.; Szalla, A. *Surf. Sci.* **2002**, *507*, 833.
27. Chen, X.; Wang, Y.; Shen, J. *Polym. Degrad. Stab.* **2005**, *87*, 527.
28. Evora, V. M. F.; Shukla, A. *Mater. Sci. Eng. A* **2003**, *361*, 358.